# Event-triggered Leader-following Formation Control for Multi-agent Systems Under Communication Faults: Application to a Fleet of Unmanned Aerial Vehicles (Special Section on FDD and FTC)

Juan Antonio Vazquez Trejo[1,2,*], Adrien Guenard[3], Manuel Adam Medina[2], Jean-Christophe Ponsart[1], Laurent Ciarletta[3], Damiano Rotondo[4], Didier Theilliol[1]

1. University of Lorraine, CRAN UMR 7039 CNRS, France.
2. TECNM/Cenidet, Electronic engineering department, Cuernavaca Morelos, Mexico.
3. Université de Lorraine, CNRS, LORIA, F-54000 Nancy, France
4. University of Stavanger, Department of Electrical and Computer Engineering (IDE), Stavanger, Norway.

**Abstract:** The main contribution of this paper is the design of an event-triggered formation control for leader-following consensus in second-order multi-agent systems (MASs) under communication faults. All the agents must follow the trajectories of a virtual leader despite communication faults considered as smooth time-varying delays dependent on the distance between the agents. Linear matrix inequalities (LMIs)-based conditions are obtained to synthesize a controller gain that guarantees stability of the synchronization error. Based on the closed-loop system, an event-triggered mechanism is designed to reduce the control law update and information exchange in order to reduce energy consumption. The proposed approach is implemented in a real platform of a fleet of unmanned aerial vehicles (UAVs) under communication faults. A video with the experimental results in this link https://youtu.be/Lo_kuGY9Wq4.

**Keywords:** Event-triggered, leader-following consensus, communication faults, formation control, unmanned aerial vehicles, experimental results.

DOI：

## 1. Introduction

Leader-following consensus for multi-agent systems (MASs) has attracted interest due to its applications in collective missions including, among others, self-organization, clusters of satellites, formation flying, and sensor networks [1]. Leader-following consensus is a particular problem in multi-agent systems where all the agent trajectories must converge to the trajectory of a leader [2]. Several research works have increased the focus on considering multiplicative and additive noises [3], switching topologies [4], time delays [5], particle swarm optimization [6], and event-triggered mechanisms [7], among others. The information exchange through digital networks

is a key point in leader-following consensus. However, delays [8], packet losses [9], communication faults [10], or bandwidth limitations [11] are challenges in real engineering applications [12].

An alternative control strategy is the event-triggered approach, which is used often for reducing the information exchange and the control law rate [13]. The difference between event-triggered and time-triggered approaches are that considers a periodic control law update, whereas, in the former, the update of the control law and the information exchange between the agents are determined by an event generator [14,15]. Related works have increased the focus on event-triggered leader-following consensus in the last decades considering sufficient conditions using the M-matrix theory and algebraic inequalities for second-order nonlinear time-delayed dynamic agents [16]; LMIs-based conditions using the M-matrix theory for reaching bipartite consensus in nonlinear second-order agents [17]; nonuniform delays in heterogeneous agents [8]; bounded delays in fractional-order agents [18]; sufficient conditions including dependent, independent fixed delays, time-varying delays [19]; constant delays in linear agents [20]. R2Q1, R3Q1 Nevertheless, the aforementioned works have not been considered a degradation in the communication based on the distances between agents. In [10], communication faults are modeled as a modification in the weights of the adjacency matrix as a result of a malfunction in the exchange of information. The communication faults in this work are considered as a delay-dependent on the distances between agents. Unlike [21], where a time-triggered control is designed to tolerate smooth communication faults, the main contribution of this paper inspired by [7], is the design of an event-triggered strategy to solve the leader-following consensus problem in second-order multi-agent systems under communication faults. A synthesis of a robust control gain is obtained in order to tolerate faults in the exchange of information. Then, based on the closed-loop system, an event-triggered mechanism is used in order to reduce the information exchange between agents and the control update rate. The proposed technique has been implemented in a real platform comprising a fleet of UAVs achieving a desired formation and following a virtual leader agent in spite of the degradation in the exchange of information.

This paper is organized as follows. Preliminaries and problem statement are provided in Section 2. The event-triggered leader-following formation control design is described in Section 3. The experimental results are shown in Section 4. Finally, the main conclusions are presented in Section 5.

# 2. Preliminaries and problem statement

## 2.1 Notation and graph theory

Given a matrix $X$, $X^T$ denotes its transpose,

$X > 0\ (< 0)$ denotes a positive (negative) definite matrix. $\|.\|$ denotes the Euclidean norm. For simplicity, the symbol $*$ within a symmetric matrix represents the symmetric entries. The Hermitian part of a square matrix $X$ is denoted by $He\{X\} = X + X^T$. The symbol $\otimes$ denotes the Kronecker product, which for real matrices $A$,$B$, $C$, and $D$ with appropriate dimensions, satisfies the following properties [22]:

1. $(A + B) \otimes C = A \otimes C + B \otimes C$,
2. $(A \otimes B)^T = A^T \otimes B^T$,
3. $(A \otimes B)(C \otimes D) = (AC) \otimes (BD)$.

A directed graph $\mathcal{G}$ is a pair $(\mathcal{V}, \mathcal{E})$, where $\mathcal{V} = \{v_1, \dots, v_N\}$ is a non-empty finite node set (set of agents) and $\mathcal{E} = \{(i,j): i,j \in \mathcal{V}\} \subseteq \mathcal{V} \times \mathcal{V}$ is an edge set of ordered pairs of $N$ nodes. The neighbors of the node $i$ are denoted as $j \in \mathcal{N}_i$. The adjacency matrix $\mathcal{A} = [a_{ij}] \in \mathbb{R}^{N\times N}$ associated with the graph $\mathcal{G}$ is defined such that $a_{ii} = 0$, $a_{ij} > 0$ if and only if $(i,j) \in \mathcal{E}$ and $a_{ij} = 0$ otherwise. The Laplacian matrix $\mathcal{L} = [\ell_{ij}] \in \mathbb{R}^{N\times N}$ of the graph $\mathcal{G}$ is defined as $\ell_{ii} = \sum_{j\neq i} a_{ij}$ and $\ell_{ij} = -a_{ij}$, $i \neq j$.

**Lemma 1 (**[23]**).** *For a given matrix* $\begin{bmatrix} S_1 & S_2 \\ S_2 & S_3 \end{bmatrix} < 0$ *the following statements are equivalent:*

1. $S_1 < 0$, $S_3 - S_2^T S_1^{-1} S_2 < 0$;
2. $S_3 < 0$, $S_1 - S_2^T S_3^{-1} S_2 < 0$.

2.2 Problem statement

Consider the second-order multi-agent system as follows:

$$\begin{aligned} \dot{p}_i(t) &= v_i(t), \\ \dot{v}_i(t) &= u_i(t), \end{aligned} \tag{1}$$

where $p_i(t)$, $v_i(t)$, $u_i(t) \in \mathbb{R}^n$ are the position, velocity, and acceleration input $\forall i = 1,2,\dots,N$, in an $n$-dimensional Euclidean space. Leader-following consensus is designed such that all the agents follow the trajectories of a virtual leader. In this case, the leader's dynamic is considered as follows:

$$\dot{p}_r(t) = v_r(t), \tag{2}$$

where $p_r(t)$, $v_r(t) \in \mathbb{R}^n$ are the position and velocity of the leader agent. The leader agent position can be manipulated through its velocity. Let us define the rigid desired-position formation from the agent $i$ to its neighbors $j$, as $h_i, h_j \in \mathbb{R}^n$. According to [1], the classical leader-following formation control is given by:

$$\begin{aligned} u_i(t) = \textstyle\sum_{j\in\mathcal{N}_i} a_{ij} \Big[\Big(\big(p_j(t) - p_i(t)\big) - \\ \big(h_j - h_i\big)\Big) + \big(v_j(t) - v_i(t)\big)\Big] - \big(p_i(t) - \\ p_r(t)\big) - \big(v_i(t) - v_r(t)\big), \end{aligned} \tag{3}$$

where $\mathcal{N}_i$ is the set of $i$'s neighbors.

***R1Q5* Assumption 1.** *The graph $\mathcal{G}$ is an undirected graph.*

**Assumption 2.** *All the agents receive information states from the virtual leader agent.*

***R1Q5 Lemma 2 (***[24]***).*** *The Laplacian matrix $\mathcal{L}$ associated with an undirected graph has at least one zero eigenvalue and all the nonzero eigenvalues are positive. The Laplacian matrix $\mathcal{L}$ has exactly one zero eigenvalue if and only if the graph is connected.*

R1Q3. Using the consensus protocol (3), the multi-agent system (1) achieves the desired formation if the following is satisfied:

$$\begin{aligned} &\lim_{t\to\infty} \big\|(p_i(t) - h_i) - \big(p_j(t) - h_j\big)\big\| = 0, \\ &\forall i \neq j,\ i = 1,2,\dots N. \end{aligned} \tag{4}$$

Bandwidth limitations, delays, or packet losses are challenges in real engineering applications in multi-agent systems. Let us define $\tau_{ij}(t)$ as the communication faults between the agent $i$ and the agent $j$. Based on $\tau_{ij}(t)$, the leader-following formation control under communication faults (3) becomes:

$$\begin{aligned} u_i(t) = \sum_{j\in\mathcal{N}_i} a_{ij} \Big[ \Big( \big(p_j\big(t-\tau_{ij}(t)\big) - p_i\big(t-\tau_{ij}(t)\big)\big) \\ - (h_j - h_i) \Big) \\ + \big(v_j\big(t-\tau_{ij}(t)\big) - v_i\big(t-\tau_{ij}(t)\big)\big) \Big] \\ - (p_i(t) - p_r(t)) - (v_i(t) - v_r(t)). \end{aligned} \quad (5)$$

A degradation of the communication between agents can be associated to their distance as considered in [25]. Communication faults are considered dependent on the agent positions in link with the distance between them and described by the following function:

$$\tau_{ij}(t) = \Big(\beta_1 - \beta_1 e^{-\beta_2 \|p_i(t) - p_j(t)\|}\Big)\Big(0.5 - 0.5\tanh\big(\beta_3(t-t_f)\big)\Big), \quad (6)$$

where $\beta_1$, $\beta_2$, and $\beta_3$ are positive constants, and $t_f$ is the time of fault occurrence.

*R1Q1* **Assumption 3.** *The derivative of the communication fault* $\dot{\tau}_{ij}(t) \le d_\tau < 1, \forall i \neq j, j \in \mathcal{N}_i$ *where* $d_\tau$ *is a fixed scalar.*

Note that, when $\tau_{ij}(t) = 0$, the leader-following formation control problem can be solved using (3). Nevertheless, as reported in [24], the longest delay to reach the consensus is determined as $\tau_{ij} < \frac{\pi}{2\lambda_N(\mathcal{L})}$, where $\lambda_N(\mathcal{L})$ is the maximum eigenvalue of the Laplacian matrix, and the delay is considered constant with the same value for all agents in a fixed, undirected, and connected graph.

The problem under consideration in this paper is to design an event-triggered leader-following formation control such that all the agents follow the leader's trajectories subject to communication faults considered as smooth delays dependent on the agent positions.

# 3. Event-triggered leader-following formation control design

In the following subsections, a time-triggered formation control design and the event-triggered mechanism are presented in order to develop a strategy such that all the agents tolerate communication faults while reducing the information exchange.

## 3.1 Time-triggered leader-following formation control design

Let us define the error between the agent $i$ and the leader as follows:

$$\begin{aligned} \bar{p}_i(t) &= p_i(t) - p_r(t), \\ \bar{v}_i(t) &= v_i(t) - v_r(t). \end{aligned} \quad (7)$$

Let $\delta_i(t) = [\bar{p}_i(t)^T - h_i^T, \bar{v}_i(t)^T]^T$, then, the error dynamics can be rewritten as follows:

$$\begin{aligned} &\dot{\delta}_i(t) = A\delta_i(t) + Bu_i(t), \\ &\text{with } A = \begin{bmatrix} 0 & I_n \\ 0 & 0 \end{bmatrix} \text{ and } B = \begin{bmatrix} 0 \\ I_n \end{bmatrix}. \end{aligned} \quad (8)$$

Adding the control gain $K_c \in \mathbb{R}^{n\times 2n}$ and the scalar $\alpha$, the leader-following control (5) is modified in order to tolerate communication faults when $\tau_{ij}(t) > \frac{\pi}{2\lambda_N(\mathcal{L})}$ as follows:

$$u_i(t) = K_c \Big[\sum_{j\in\mathcal{N}_i} a_{ij} \Big(\delta_i\big(t-\tau_{ij}(t)\big) -$$

$$\delta_j\left(t-\tau_{ij}(t)\right)\Big)+\alpha\delta_i(t)\Big], \quad (9)$$

where $K_c$ is the control gain to be designed and $\alpha > 0$ must be a positive constant which represents the relationship between the leader and the followers. Based on (8), (7) becomes:

$$\dot{\delta}_i(t) = A\delta_i(t) + BK_c\Big[\sum_{j\in N_i} a_{ij}\Big(\delta_i\left(t-\tau_{ij}(t)\right) - \delta_j\left(t-\tau_{ij}(t)\right)\Big) + \alpha\delta_i(t)\Big], \quad (10)$$

Let $\delta(t) = [\delta_1(t)^T, \delta_2(t)^T, \dots, \delta_N(t)^T]^T$ and $\delta(t-\tau) = \Big[\delta_1\left(t-\tau_{1j}(t)\right)^T, \delta_2\left(t-\tau_{2j}(t)\right)^T, \dots, \delta_N\left(t-\tau_{Nj}(t)\right)^T\Big]^T$, then the error dynamics (9) are rewritten as follows:

$$\dot{\delta}(t) = \big(I_N \otimes (A + \alpha BK_c)\big)\delta(t) + (\mathcal{L} \otimes BK_c)\delta(t-\tau), \quad (11)$$

The following theorem provides LMI-based conditions for the computation of the control gain $K_c$.

**Theorem 1.** *Given the non-zero eigenvalues of the Laplacian matrix $\lambda_i(\mathcal{L}), i = 2,3,\dots,N$, scalars $\alpha > 0$, $\mu_1 > 0$, $\mu_2 > 0$, and $\dot{\tau}_{ij} \le d_\tau < 1$, the leader-following consensus is quadratically stable under (9), if there exist symmetric matrices $P_1 > 0$, $P_2 > 0$, and a matrix $K_c$ such that the following inequality*

$$\begin{bmatrix} Q_1 & 0 & Q_{2i} & Q_3 \\ * & Q_4 & -\mu_2 K_c^T & 0 \\ * & * & -2\mu_2 I & 0 \\ * & * & * & -I \end{bmatrix} < 0 \quad (12)$$

*holds $\forall i = 2,3,\dots,N$, with $Q_1 = He\{P_1 A\} + I - \frac{2P_1}{\mu_1} + P_2$, $Q_{2i} = -\lambda_i P_1 B$, $Q_3 = \frac{P_1}{\mu_1} + \mu_1\alpha BK_c$, $Q_4 = -(1-d_\tau)P_2$.*

***Proof.*** Let us define the following candidate R1Q6 Lyapunov functional inspired by [26]:

$$V = \delta(t)^T(I_N \otimes P_1)\delta(t) + \int_{t-\tau}^{t} \delta(s)^T(I_N \otimes P_2)\delta(s)ds. \quad (13)$$

The time derivative of $V$ along any solution of the system (11) is given by:

$$\dot{V} = 2\delta(t)^T(I_N \otimes P_1)\dot{\delta}(t) + \delta(t)^T(I_N \otimes P_2)\delta(t) - (1-\dot{\tau})\delta(t-\tau)^T(I_N \otimes P_2)\delta(t-\tau). \quad (14)$$

According to [26] and Assumption 3, (14) is negative-definite when

$$\dot{V} = 2\delta(t)^T(I_N \otimes P_1)\dot{\delta}(t) + \delta(t)^T(I_N \otimes P_2)\delta(t) - (1-d_\tau)\delta(t-\tau)^T(I_N \otimes P_2)\delta(t-\tau) < 0, \quad (15)$$

thus,

$$\dot{V} = 2\delta(t)\text{^}T\ (I\_N \otimes (P\_1\ (A + \alpha P\_1\ BK\_c\ )))\delta(t) + 2\delta(t)\text{^}T\ (\mathcal{L} \otimes P\_1\ BK\_c\ )\delta(t-\tau) + \delta(t)\text{^}T\ (I\_N \otimes P\_2\ )\delta(t) - (1 - d\_\tau\ )\delta(t-\tau)\text{^}T\ (I\_N \otimes P\_2\ )\delta(t-\tau) < 0. \quad (16)$$

Let us perform a spectral decomposition of the Laplacian matrix $\mathcal{L}$, such that $\mathcal{L} = TJT^{-1}$ with an invertible matrix $T \in \mathbb{R}^{N\times N}$ and a diagonal matrix $J = diag(\lambda_1 = 0, \lambda_2, \dots, \lambda_N)$. R1Q7 By Lemma 2, eigenvalues of $\mathcal{L}$ form a base of eigenvectors which are used to construct the

invertible matrix $T$. Let us define the following change of coordinates:

$$\psi(t) = (T^{-1} \otimes I_N)\delta(t),$$
$$\psi(t-\tau) = (T^{-1} \otimes I_N)\delta(t-\tau). \quad (17)$$

Replacing (17) in (16) leads to:

$$\dot{V} = 2\psi(t)^T \Big(I_N \otimes \big(P_1(A + \alpha BK_c)\big)\Big)\psi(t) + 2\psi(t)^T (J \otimes P_1 BK_c)\psi(t-\tau) + \psi(t)^T (I_N \otimes P_2)\psi(t) - (1-d_\tau)\psi(t-\tau)^T (I_N \otimes P_2)\psi(t-\tau). \quad (18)$$

By Lemma 2, it is obtained that $\psi_1(t) = 0$ and $\psi_1(t-\tau) = 0$ due to $\lambda_1 = 0$, then (18) is rewritten as follows:

$$\dot{V} = \sum_{i=2}^{N} \psi_i(t)^T He\{P_1(A + \alpha BK_c)\}\psi_i(t) + 2\sum_{i=2}^{N} \psi_i(t)^T \lambda_i P_1 BK_c \psi_i(t-\tau) + \sum_{i=2}^{N} \psi_i(t)^T P_2 \psi_i(t) - (1-d_\tau)\sum_{i=2}^{N} \psi_i(t-\tau)^T P_2 \psi_i(t-\tau). \quad (19)$$

Then, the following matrix is obtained:

$$\dot{V} = \sum_{i=2}^{N} \begin{bmatrix} \psi_i(t)^T \\ \psi_i(t-\tau)^T \end{bmatrix}^T \Omega_i \begin{bmatrix} \psi_i(t) \\ \psi_i(t-\tau) \end{bmatrix},$$
$$\Omega_i = \begin{bmatrix} He\{P_1(A + \alpha BK_c)\} + P_2 & \lambda_i P_1 BK_c \\ * & -(1-d_\tau)P_2 \end{bmatrix}. \quad (20)$$

If matrix $\Omega_i < 0, \forall i = 2,3,\dots,N$, then $\dot{V} < 0$; thus, the synchronization error between the leader and the followers is quadratically stable. R1Q4 Using Schur complement (Lemma 1) in (12), the following inequality is obtained:

$$\begin{bmatrix} R_1 & 0 & Q_{2i} \\ * & Q_4 & -\mu_2 K_c^T \\ * & * & -2\mu_2 I \end{bmatrix} < 0, \quad (21)$$

where $R_1 = He\{P_1 A\} + I - \frac{2P_1}{\mu_1} + P_2 + \left(\frac{P_1}{\mu_1} + \mu_1 \alpha BK_c\right)^T \left(\frac{P_1}{\mu_1} + \mu_1 \alpha BK_c\right)$. The inequality (21) is pre- and post- multiplied by $\begin{bmatrix} I & 0 & 0 \\ 0 & I & -K_c^T \end{bmatrix}$ and its transpose, thus obtaining:

$$\begin{bmatrix} R_1 & Q_{2i} \\ * & Q_4 \end{bmatrix} < 0, \quad (22)$$

Note that:

$$He\{P_1(A + \alpha BK_c)\} + P_2 \leq He\{P_1(A + \alpha BKc)\} + P_2 + \alpha^2 (P_1 BK_c)^T (P_1 BK_c) = He\{P_1 A\} + P_2 - \frac{P_1^2}{\mu_1^2} + \left(\frac{P_1}{\mu_1} + \alpha BK_c\right)^T \left(\frac{P_1}{\mu_1} + \alpha BK_c\right), \quad (23)$$

where $\mu_1 > 0$. By taking into account the following inequality:

$$\left(I - \frac{P_1}{\mu_1}\right)\left(I - \frac{P_1}{\mu_1}\right) \geq 0,$$
$$I - \frac{2P_1}{\mu_1} \geq -\frac{P_1^2}{\mu_1^2}, \quad (24)$$

and combining (23) and (24), the following is obtained:

$$He\{P_1(A + \alpha PBK_c)\} + P_2 \leq He\{P_1 A\} + I + P_2 - \frac{2P_1}{\mu_1} + \left(\frac{P_1}{\mu_1} + \alpha BK_c\right)^T \left(\frac{P_1}{\mu_1} + \alpha BK_c\right). \quad (25)$$

Based on (25) and (22), $\Omega_i < 0$ is recovered,

thus, the LMI (12) corresponds to (20) and the synchronization error is quadratically stable

under (9), thus completing the proof. ■

***Remark 1:*** *Theorem 1 guarantees the time-triggered leader-following formation control design which is continuously updated.*

3.2 Event-triggered mechanism

The following section, an event-triggered mechanism is developed in order to reduce the information exchange and the control update rate.

The update of the control law action in event-triggered approaches depends on an event error. This event error is calculated based on the last and the current state values. When the magnitude of the event error exceeds a threshold, the control law value is updated, otherwise, the control law keeps the last calculated value. The control in (9) is modified in order to design an event-triggered mechanism as follows:

$$u_i(t) = K_c \left[\sum_{j\in\mathcal{N}_i} a_{ij} \left(\delta_i\left(t_k^i - \tau_{ij}(t_k^i)\right) - \delta_j\left(t_k^i - \tau_{ij}(t_k^i)\right)\right) + \alpha\delta_i(t_k^i)\right], \quad (26)$$

where $\delta_i(t_k^i)$ and $\delta_j(t_k^i)$ are the last values of the synchronization errors of agents $i$ and $j$, respectively, and agent $j$; $\delta_i\left(t_k^i - \tau_{ij}(t_k^i)\right)$ and $\delta_j\left(t_k^i - \tau_{ij}(t_k^i)\right)$ are the last values of the delayed synchronization errors of agents $i$ and $j$. The sequence of event-times $0 \le t_0^i \le t_1^i \ldots$ of the agent $i$ is defined as $t_{k+1}^i = \inf\{t: t > t_k^i, f_i(\zeta_i(t)) > 0\}$. The agent $i$ requests the information of the agent $j$ at the event $t_{k+1}^i$ in order to update the control law, otherwise, the control law keeps the last computed value. Let us define the event error as follows:

$$\zeta_i(t) = \delta_i(t_k^i) - \delta_i(t),$$
$$\zeta_i\left(t - \tau_{ij}(t)\right) = \delta_i\left(t_k^i - \tau_{ij}(t_k^i)\right) - \delta_i\left(t - \tau_{ij}(t)\right). \quad (27)$$

According to [7], if the leader-following consensus is quadratically stable, then, the following event function can be considered:

$$f_i(t) = \|\zeta_i(t)\| - (c_1 + c_2 e^{-c_3 t}), \quad (28)$$

where $c_1 > 0$, $c_2 > 0$, $0 < c_3 < |\gamma_{min}(A + \alpha BK_c)|$, and $\gamma_{min}(A + \alpha BK_c)$ is the minimum eigenvalue of $(A + \alpha BK_c)$.

# 4. Example: Fleet of UAVs under communication faults

In order to illustrate the effectiveness of the proposed strategy, real implementations in a fleet of UAVs are presented in the following section.

The experimental platform is described and some experimental results are shown in the following section. A video corresponding to the results can be found at the following link https://youtu.be/Lo_kuGY9Wq4.

4.1 Experimental platform description

The experimental platform used for this implementation consists of: an Optitrack system to recognize the UAVs in a three-dimensional space by image processing using cameras Prime 17W; motive 2.1.1 is the

software to manipulate the Optitrack which uses VRPN protocol with communication to a virtual machine; Ubuntu 16.04 is installed in the virtual machine with ROS Kinetic to manipulate the UAVs in parallel with Motive; identical Bebop 2 parrot are the UAVs (see Fig. 1). The code is developed in Python 2.7. The sample time is 0.02s.

*Fig. 1 Bebop 2 parrot*

According to [27], a fleet of UAVs can be described as a second-order multi-agent system if an inner closed-loop control is considered for each UAV employing their angles with the following references:

$$\begin{aligned}
&\psi_{d_i}(t) = 0,\\
&\theta_{d_i}(t) = \arctan\left(\frac{u_{x_i}}{u_{z_i}+g}\right),\\
&\phi_{d_i}(t) = \arcsin\left(-\frac{u_{y_i}}{\sqrt{u_{x_i}^2+u_{y_i}^2+\left(u_{z_i}+g\right)^2}}\right),\\
&T_i(t) = m_s\sqrt{u_{x_i}^2+u_{y_i}^2+\left(u_{z_i}+g\right)^2},
\end{aligned} \tag{29}$$

where $u_i(t) = \left[u_{x_i}, u_{y_i}, u_{z_i}\right]^T$ is the consensus control law calculated using (5) (classical formation control $K_c = [-I \quad -I]$), (9) (time-triggered robust approach), and (27) (event-triggered approach); $\psi_{d_i}(t)$, $\theta_{d_i}(t)$, and $\phi_{d_i}(t)$ are the reference angles for each UAV; $m_s = 0.5Kg$ is the mass of the UAV, which are considered to be homogeneous; $g = 9.806\frac{\mathrm{m}}{\mathrm{s}^2}$ is the acceleration of gravity.

The goal of the 3 UAVs is to form an isosceles triangle and follow the trajectories of a virtual agent with the following desired formation $h_1[0,0]^T$, $h_2 = [0,1.5]^T$, and $h_3 = [0.75,1.3]^T$.

The LMI in Theorem 1 is solved with the following parameters: $\mu_1 = 1$, $\mu_2 = 10$, $\alpha = 1$, and $d_\tau = 0.2$ obtaining the control gain $K_c = [\,-(0.4922\,)I_3 \quad -(0.9768)I_3\,]$. This control gain is used in both the time-triggered and event-triggered approach. R3Q3 Table 1 shows the initial values of the UAVs.

Table 1 Initial conditions of the UAVs

| Agent | Position $[x, y]$ | Velocity |
|---|---|---|
| 1 | [-0.7249, -0.7232] | [-0.0084, 0.0357] |
| 2 | [0.0330, -0.3345] | [0.0129, -0.0107] |
| 3 | [1.5115, 1.0167] | [-0.0239, 0.0082] |

The communication topology is described by the following Laplacian matrix:

$$\mathcal{L} = \begin{bmatrix} 2 & -1 & -1 \\ -1 & 2 & -1 \\ -1 & -1 & 2 \end{bmatrix}. \tag{30}$$

The communication fault is implemented through an artificial function with the following parameters: $\beta_1 = 0.8$, $\beta_2 = 1$, $\beta_3 = 0.6$, and $t_f = 10s$. All the UAVs are affected by the communication fault. The event-function has the following parameters: $c_1 = 0.03$, $c_2 = 3$, and $c_3 = 0.1$.

Three implementations have been carried out for comparing the performance of the classical formation control (5), the time-triggered robust approach (9), and the event-triggered approach (27). In the case of the classical formation control, the experiment had to be stopped to avoid the UAVs to crash.

4.2 Experimental results

Fig. 2 illustrates the obtained trajectories of the UAVs using the classical formation control.

The UAVs should follow the trajectory of the virtual agent in black, however, due to the communication faults, they start to oscillate, so they cannot maintain the formation.

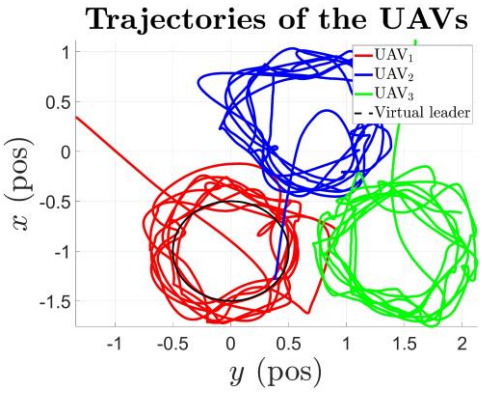


*Fig. 2 Trajectories of the UAVs (Classical approach).*

Fig. 3 shows the UAVs trajectories obtained using the time-triggered robust control. The UAVs present a decrease in the oscillations with respect to the previous case. Moreover, they maintain the desired formation.

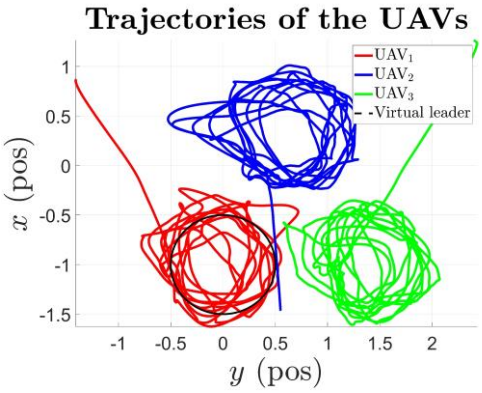


*Fig. 3 Trajectories of the UAVs (Time-triggered proposed approach)*

Fig. 4 presents the UAVs trajectories when the event-triggered mechanism is used. The UAVs present a better performance, maintaining the formation despite the communication faults.

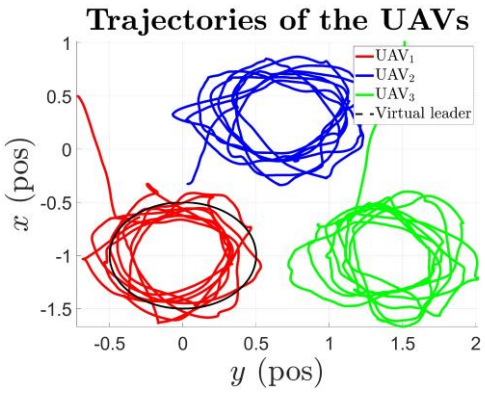


*Fig. 4 Trajectories of the UAVs (Event-triggered proposed approach)*

Fig. 5 presents the UAVs velocities obtained using the classical formation control. After approximately 140s, the UAVs start to show stronger oscillations. As mentioned earlier, in order to preserve the integrity of the UAVs, the experiment had to be stopped.

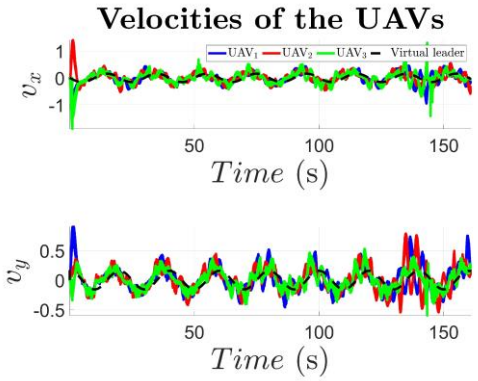


*Fig. 5 Velocities of the UAVs (Classical approach)*

Fig. 6 shows the UAVs' velocities using the time-triggered robust control. The oscillations decrease when compared to the classical formation control. However, there is still a small offset between the leader velocities and the velocities of the UAVs. Also, an offset is observed induced by the fact that the control gain is smaller than in the classical formation control.

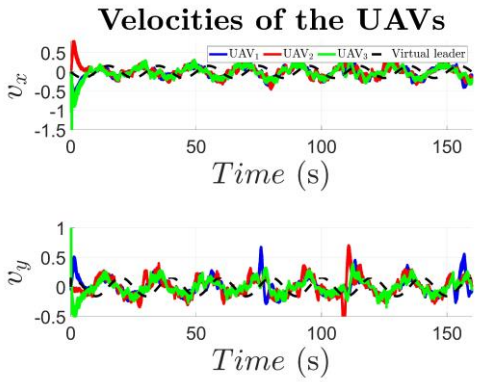


*Fig. 6 Velocities of the UAVs (Time-triggered proposed approach)*

Fig. 7 illustrates the UAVs' velocities using the event-triggered control. The oscillations are smaller compared to the other two approaches. However, the offset is still present due to the control gain. It is worth highlighting that the event-triggered control reduces the information exchange between the agents and the update rate of the control law.

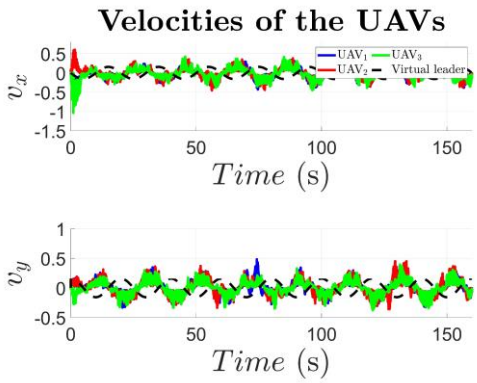


*Fig. 7 Velocities of the UAVs (Event-triggered proposed approach)*

Fig. 8 presents the event-triggered control law. The time interval between 15s and 17 s is zoomed to illustrate when the control law keeps the last value.

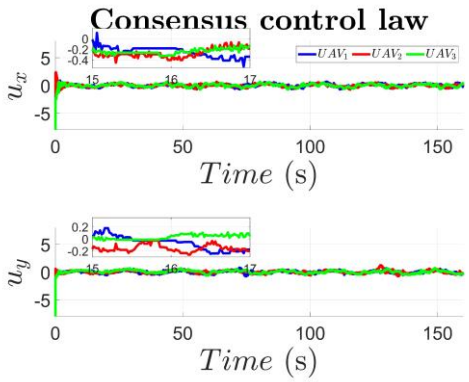


*Fig. 8 Consensus control law (Event-triggered proposed approach)*

In order to measure the performance of the consensus, let us define $d_{ij} = \|\bar{x}_i - \bar{x}_j\|$, where $\bar{x}_i = [p_i - h_i, v_i]^T$, and $\bar{x}_j = [p_j - h_j, v_j]^T$. Fig. 9 illustrates the evaluation of the performance of the consensus using the classical formation control. The performance presents oscillations after 140s due to the communication faults.

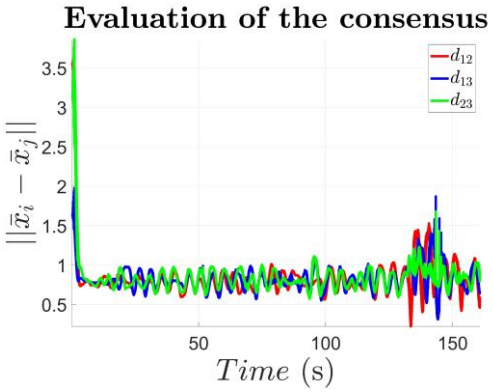


*Fig. 9 Evaluation of the consensus' performance (Classical approach)*

Fig. 10 shows the evaluation of the performance of the consensus using the time-triggered robust control. Compared to Fig. 9, the performance has been improved.

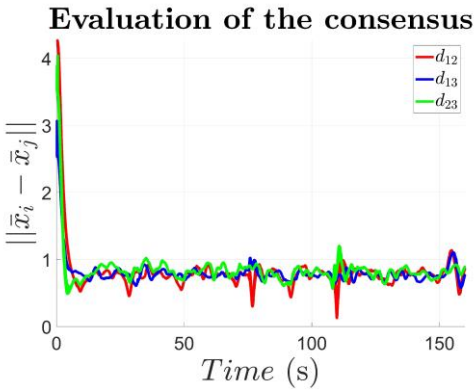


*Fig. 10 Evaluation of the consensus' performance (Time-triggered proposed approach)*

Fig. 11 presents the evaluation of the consensus performance using the event-triggered control. Compared to Fig. 10, the performance is smaller than the threshold value 1 due to the desired formation.

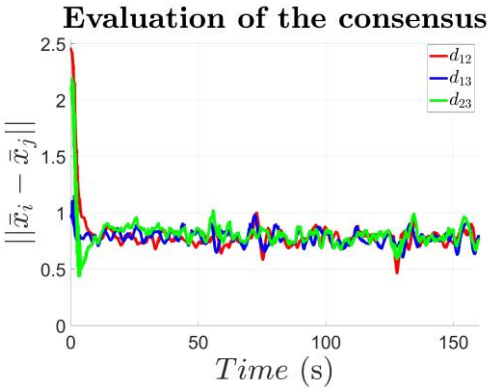


*Fig. 11 Evaluation of the consensus' performance (Event-triggered proposed approach)*

Fig. 12 presents the profile of the events for the event-triggered control. It is considered 1 for the UAV one, 2 for the UAV two, 3 for the UAV three if an event occurs, respectively, and 0 if there is not an event. A zoom is considered in some intervals in order to show when an event occurs.

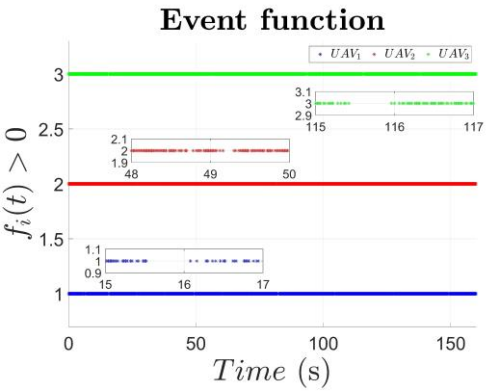


*Fig. 12 Events for updating the control law.*

R1Q8. Fig. 13 shows the total number of events in each UAV. "No event" means that the control law and the exchange of information are not updated. For example, $UAV_1$ has 1907 of no events compare with 6556 events. In contrast with time-triggered, the update of the information and the control law has been reduced.

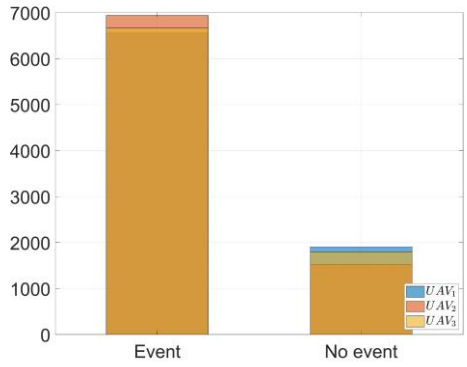


*Fig. 13Total number of events in each UAV.*

In order to quantify the performance between the approaches, root mean square (RMS) metric is used. In Table 2, the RMS value of $d_{ij}$ is presented for each combination of UAVs corresponding to the classical formation control, the time-triggered robust control, and the event-triggered control.

Table 2 Comparative of the consensus RMS

| $d_{ij}$ | Classical | Time-triggered | Event-triggered |
|---|---|---|---|
| $d_{12}$ | 0.9129 | 0.8947 | 0.8932 |
| $d_{13}$ | 0.9060 | 0.8910 | 0.8818 |

| | | | |
|---|---|---|---|
| $d_{23}$ | 0.9189 | 0.9088 | 0.8978 |

It should be noted that the event-triggered approach reduces the energy consumption.

## 5. Conclusions

This paper has presented an event-triggered formation for second-order multi-agent systems under communication faults. The controller gain has been calculated using LMI tools and an event-triggered mechanism has been introduced to reduce the information exchange between agents. The proposed approach has been implemented in a real platform of a fleet of UAVs subject to communication faults. A comparison between a state-of-the-art technique and the proposed technique has been provided, demonstrating the performance improvement brought by the proposed approach. R1Q8. For future work, a measurement of the energy consumption can be implemented in the real platform in order to compare the performance between the approaches.

## Acknowledgment

The Creativlab platform has been co-funded by state-region project contracts (CPER) "Cyberentreprises", the European Union under the "Feder-FSE Lorraine et Massif des Vosges 2014-2020", and Grand Est region.

## References

[1] Z. Li and Z. Duan, "*Cooperative control of multi-agent systems: a consensus region approach"*. CRC Press, 2014.

[2] W. Ni and D. Cheng, "Leader-following consensus of multi-agent systems under fixed and switching topologies," *Systems & Control Letters*, vol. 59, no. 3, pp. 209–217, 2010.

[3] Y. Zhang, R. Li, W. Zhao, and X. Huo, "Stochastic leader-following consensus of multi-agent systems with measurement noises and communication time-delays," *Neurocomputing*, vol. 282, pp. 136–145, 2018.

[4] B. Cui, C. Zhao, T. Ma, and C. Feng, "Leaderless and leader-following consensus of multi-agent chaotic systems with unknown time delays and switching topologies," *Nonlinear Analysis: Hybrid Systems*, vol. 24, pp. 115–131, 2017.

[5] J. Jiang and Y. Jiang, "Leader-following consensus of linear time-varying multi-agent systems under fixed and switching topologies," *Automatica*, vol. 113, p. 108804, 2020.

[6] A. Belkadi, L. Ciarletta, and D. Theilliol, "Particle swarm optimization method for the control of a fleet of Unmanned Aerial Vehicles," *Journal of Physics: Conference Series*, vol. 659, p. 012015, Nov. 2015.

[7] J. A. Vazquez Trejo, D. Rotondo, M. Adam Medina, and D. Theilliol, "Observer-based event-triggered model reference control for multi-agent systems," in *2020 International Conference on Unmanned Aircraft Systems (ICUAS)*, 2020, pp. 421–428.

[8] C. Deng, W.-W. Che, and Z.-G. Wu, "A dynamic periodic event-triggered approach to consensus of heterogeneous linear multiagent systems with time-varying communication delays," *IEEE Transactions on Cybernetics*, vol. 51, no. 4, pp. 1812-1821, 2021.

[9] Z. Wang, F. Yang, D. W. C. Ho, and X. Liu, "Robust H∞ control for networked systemswith random packet losses," *IEEE Transactions on Systems, Man, and Cybernetics, Part B (Cybernetics)*, vol. 37, no. 4, pp. 916–924, 2007.

[10] C. Chen, K. Xie, F. L. Lewis, S. Xie, and R. Fierro, “Adaptive synchronization of multi-agent systems with resilience to communication link faults,” *Automatica*, vol. 111, p. 108636, 2020.

[11] D. Liu and G. Yang, “A dynamic event-triggered control approach to leader-following consensus for linear multiagent systems,” *IEEE Transactions on Systems, Man, and Cybernetics: Systems*, pp. 1–9, 2020.

[12] M. G. Losada, "*Contributions to networked and event-triggered control of linear systems*". Springer, 2016.

[13] G. S. Seyboth, D. V. Dimarogonas, and K. H. Johansson, “Event-based broadcasting for multi-agent average consensus,” *Automatica*, vol. 49, no. 1, pp. 245–252, 2013.

[15] J. Lunze, "*Control theory of digitally networked dynamic systems”*, vol. 1. Springer, 2014.

[14] R. Obermaisser, *“Event-triggered and time-triggered control paradigms”*, vol. 22. Springer Science & Business Media, 2004.

[16] Y. Wang, J. Cao, H. Wang, and F. E. Alsaadi, “Event-triggering consensus for second-order leader-following multiagent systems with nonlinear time-delayed dynamics,” *International Journal of Control, Automation and Systems*, vol. 18, no. 5, pp. 1083–1093, 2020.

[17] J. Ren, S. Qiang, Y. Gao, and G. Lu, “Leader-following bipartite consensus of second-order time-delay nonlinear multi-agent systems with event-triggered pinning control under signed digraph,” *Neurocomputing*, vol. 385, pp. 186–196, 2020.

[18] Y. Yanyan and S. Housheng, “Leader-following consensus of general linear fractional-order multiagent systems with input delay via event-triggered control,” *International Journal of Robust and Nonlinear Control*, vol. 28, no. 18, pp. 5717–5729, 2018.

[19] X. Tan, J. Cao, X. Li, and A. Alsaedi, “Leader-following mean square consensus of stochastic multi-agent systems with input delay via event-triggered control,” *IET Control Theory & Applications*, vol. 12, no. 2, pp. 299–309, 2017.

[20] Y. Cai, H. Zhang, J. Zhang, and H. Qiang, “Distributed bipartite leader-following consensus of linear multi-agent systems with input time delay based on event-triggered transmission mechanism,” *ISA Transactions*, vol. 100, pp. 221–234, 2020.

[21] J. A. Vazquez Trejo, D. Theilliol, M. Adam Medina, C. D. Garcia Beltran, and M. Witczak, “Leader-Following Formation Control for Networked Multi-agent Systems Under Communication Faults/Failures,” in *Korbicz J., Patan K., Luzar M. (eds) Advances in Diagnostics of Processes and Systems. Studies in Systems, Decision and Control,* Springer, Cham, vol. 313, pp. 45–57,2021.

[22] A. N. Langville and W. J. Stewart, “The Kronecker product and stochastic automata networks,” *Journal of Computational and Applied Mathematics*, vol. 167, no. 2, pp. 429–447, 2004.

[23] K. Zhou and J. C. Doyle, "*Essentials of robust control”*, vol. 104. Prentice hall Upper Saddle River, NJ, 1998.

[24] R. Olfati-Saber and R. M. Murray, “Consensus problems in networks of agents with switching topology and time-delays,” *IEEE Transactions on Automatic Control*, vol. 49, no. 9, pp. 1520–1533, 2004.

[25] J.-P. Georges, D. Theilliol, V. Cocquempot, J.-C. Ponsart, and C. Aubrun, “Fault tolerance in networked control systems under intermittent observations,” *International Journal of Applied*

*Mathematics and Computer Science*, vol. 21, no. 4, pp. 639–648, 2011.

[26] Jong Hae Kim and Hong Bae Park, "H∞ state feedback control for generalized continuous/discrete time-delay system," *Automatica*, vol. 35, pp. 1443–1451, 1999.

[27] J. F. Guerrero-Castellanos, A. Vega-Alonzo, S. Durand, N. Marchand, V. R. Gonzalez-Diaz, J. Castañeda-Camacho, and W. F. Guerrero-Sánchez, "Leader-Following Consensus and Formation Control of VTOL-UAVs with Event-Triggered Communications," Sensors, vol. 19, no. 24, p. 5498, 2019.

## Biographies

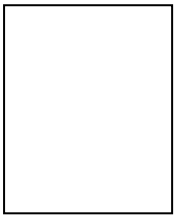

**VAZQUEZ TREJO Juan Antonio** was born in 1990. He earned his Computer Systems Engineering bachelor's degree at the Technological Institute of Zacatepec (August 2009 – December 2013, Zacatepec, Morelos, México). He received the master's degree in Automatic control at the National Research and Technological Development (CENIDET) in August 2017. Nowadays, he is pursuing a Ph.D. degree in automatic control CENIDET and the University of Lorraine. His current research interest includes multi-agent systems and fault-tolerant control. E-mail: *juan-antonio.vazquez-trejo@univ-lorraine.fr*

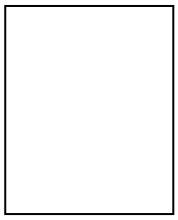

**GUENARD Adrien** E-mail: *adrien.guenard@loria.fr*

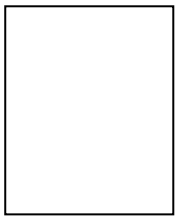

**ADAM-MEDINA Manuel** E-mail: *manuel.am@cenidet.tecnm.mx*

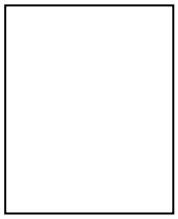

**PONSART Jean-Christophe** E-mail: *jean-christophe.ponsart@univ-lorraine.fr*

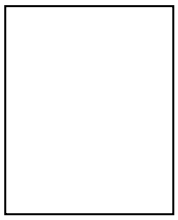

**CIARLETTA** Laurent E-mail: *laurent.ciarletta@loria.fr*

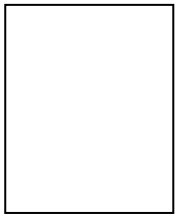

**ROTONDO** Damiano received the PhD degree from the Polytechnic University of Catalonia, Spain, in 2016. Since February 2020, he has been an Associate Professor at the University of Stavanger, Norway. His main research interests include gain-scheduled control systems, fault detection

and isolation (FDI), and fault tolerant control (FTC). E-mail: *damiano.rotondo@uis.no*

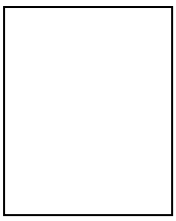

**THEILLIOL Didier** E-mail: *didier.theilliol@univ-lorraine.fr*